THE RESIDUAL STRENGTH OF A 2.5 m WIDE BUSHVELD MERENSKY REEF CRUSH PILLAR

B P Watson, S M Mosomane, J S Kuijpers and D P Roberts
CSIR, Natural Resources and the Environment

Abstract

The first crush pillars on the Bushveld Platinum mines were introduced at Union Section in 1978. Before the introduction of crush pillars, serious problems were experienced when stoping advanced to a point 30 m to 40 m on both sides of the centre gully. At least three to four stopes were collapsing per month. The introduction of the pillars stopped the stope collapses in the mining area where they were introduced. The residual strengths in these pillars were never measured, however the successful elimination of the "back-break" problem suggests that the original pillars had a residual strength of at least 8 MPa. Apart from back analyses, very little work has been done to determine the residual strength of crush pillars and only very recently have any measurements been made. The lack of knowledge in this field has resulted in pillars being designed based on experience. Concerns regarding stope collapses, similar to the Coalbrook disaster, have led to larger pillars being cut in more recent times. If such pillars were cut in brittle quartzites they would always fail violently but the ductile nature of the Merensky Reef generally allows large pillars to fail without bursting. Occasionally, however, one would burst in a working area. Increased incidence of bursting has been reported on some mines at deeper levels but most of these bursts occur in the back areas. Nevertheless, the incidence of bursting increases the risk of falls of ground in already dangerous areas, and the larger pillars decrease the extraction ratio. This paper describes the evaluation of stress measurements conducted in two boreholes over a crush pillar with dimensions 2.5 m x 4.0 m, and a height of 1.2 m. Boussinesq equations for vertical and shear stress were used to analyse the original measurements and provide a stress profile across the pillar as well as the residual strength of the pillar. The results showed an unexpectedly high peak stress of 280 MPa at the centre of the pillar and a residual strength of 48 MPa. The reason for the high residual strength is suspected to be the result of the stiff environment under which the pillar failed and the small height of the siding on the up-dip edge of the pillar. More measurements should be conducted on several mines to establish a range of residual strengths for narrow crush pillars.

1 Introduction

Crush pillars were introduced to the mining industry at Union Section by Korf[1] in 1978 to stop a serious "back break" (stope collapse) problem where at least three to four stopes were collapsing per month. Difficulties were experienced when stoping advanced to a point 30 m to 40 m on both sides of the centre gully. Sudden failure of the beam frequently occurred at this stage, resulting in parting of the rock at the bottom contact of the Bastard Reef some 20 m above the stopes. The pillars that were introduced had dimensions of 1.5 m x 3 m and a height of about 1 m. Although the pillars had obviously failed (crushed) near the working face, the introduction of these pillars stopped the stope collapses in the mining area where they were

used. This area extended from 100 m to 700 m below surface and about 1300 m along strike. Today the use of these "crush" pillars is widespread across the Platinum industry in the form of small in-stope chain pillars oriented either on strike for breast mining (see Figure 1) or on dip for up or down dip mining.

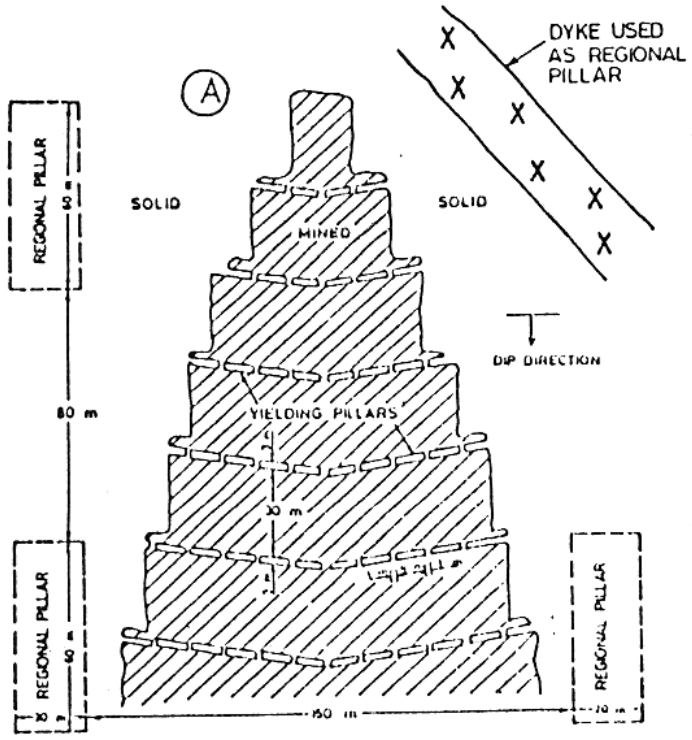

Figure 1 Plan view of a typical breast stope

The residual stresses in the original pillars were never measured, but the successful elimination of the backbreak problem suggests that the original pillars had a residual strength of at least 8 MPa. Back-analysis performed by Roberts et al[2] estimated the residual strength of normal sized crush pillars to be about 20 MPa. These analyses were backed up with *in situ* measurements made by the doorstopper strain relief method over two adjacent pillars. The results indicated residual strengths of about 18 MPa. A support resistance of 500 kN/m2 is required to stabilize the Bastard Reef contact at 20 m above the stope, which translates into a pillar strength requirement of 9 MPa. The uncertainties regarding the residual strength of crush pillars, driven mainly by a lack of knowledge, has resulted in larger pillars being cut in more recent times to avoid a disaster similar to Coalbrook. Intuitively, larger pillars are stronger than narrower pillars since the failed material around the outside of the wider pillar provides more confinement to the centre core than a narrower pillar. Oversize pillars, however, have a greater tendency to fail violently because the higher strength means that failure occurs at some distance from the stiff face under soft loading conditions. Such pillars cut in brittle quartzites always fail violently. However, the ductile nature of the Merensky Reef generally allows large

pillars to accommodate failure without bursting, but occasionally one would burst in a working area as shown in Figure 2. Increased incidence of bursting has been reported on some mines at deeper levels but most of these occur in the back areas.

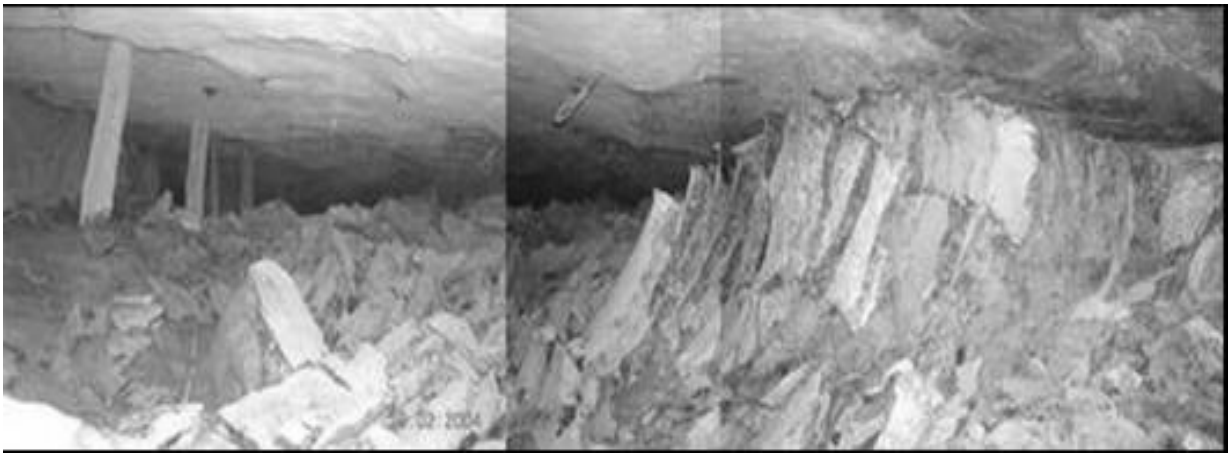

Figure 2 Panoramic view showing the up-dip end of a burst pillar. Note the gully is full of rock fragments from the pillar burst

The additional seismicity resulting from these pillar bursts increases the risk of falls of ground (FOG) in already dangerous areas. Unnecessarily large pillars also waste precious resources. The importance of proper crush pillar design is clear.

Crush pillar behaviour is described in Watson et al[3]. This paper therefore only describes the analysis of in situ measurements conducted over a pillar after failure had taken place. The dimensions of the pillar in the case study are 2.5 m x 4.0 m, with a height of 1.2 m, i.e. a width:height ratio of 2.1:1.

2 Site description

The instrumentation was installed in a Merensky Reef stope approximately 1100 m below surface. A breast mining configuration was used as shown in Figure 3, with the down-dip face being advanced ahead of the up-dip face. The mining configuration at the time of the measurements is shown in the figure.

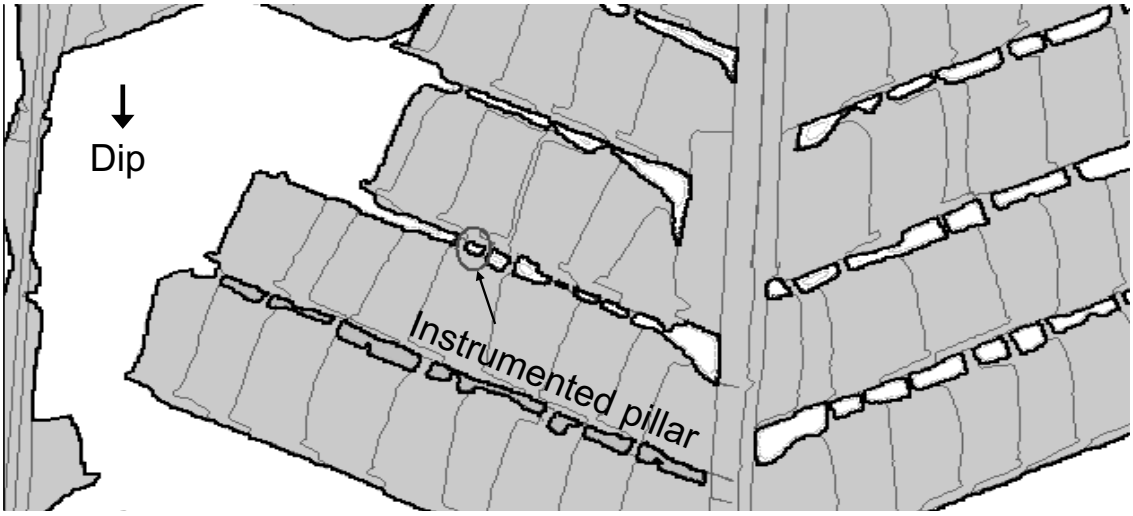

Figure 3 Plan showing the instrumentation site. The instrumented pillar is highlighted. Reef dipping at 10

In situations where the down-dip face is mined ahead of the up-dip panel, it is important to ensure that sidings are carried close to the face. Dangerous conditions could be created when a wide pillar is made narrower by cutting the siding when the pillar is some distance away from the stiff face support. This condition was avoided in the instrumented pillar by mining the siding from the advanced strike gully (ASG) ahead of the face (see Figure 4). Thus the pillar failed in a very stiff environment.

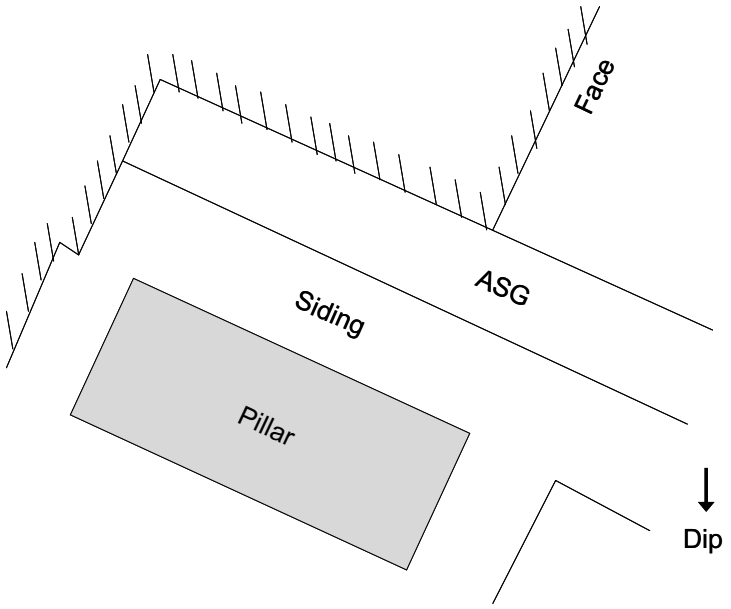

Figure 4 Mining configuration around the instrumented pillar at formation

3 Instrumentation

A total of 12 stress measuring instruments were installed in two boreholes drilled into the hangingwall of the pillar (see Figure 5). In plan the boreholes were drilled across the narrow section of the pillar from the centre of the long axis (see Figure 6). Nine biaxial cells (Doorstoppers) and one CSIR triaxial cell were installed in a shallow-dipping borehole (15° steeper than the reef), drilled from the down-dip panel. The shallow dip of the borehole ensured that the stress was measured in a plane almost perpendicular to the pillar as shown in Figure 7.

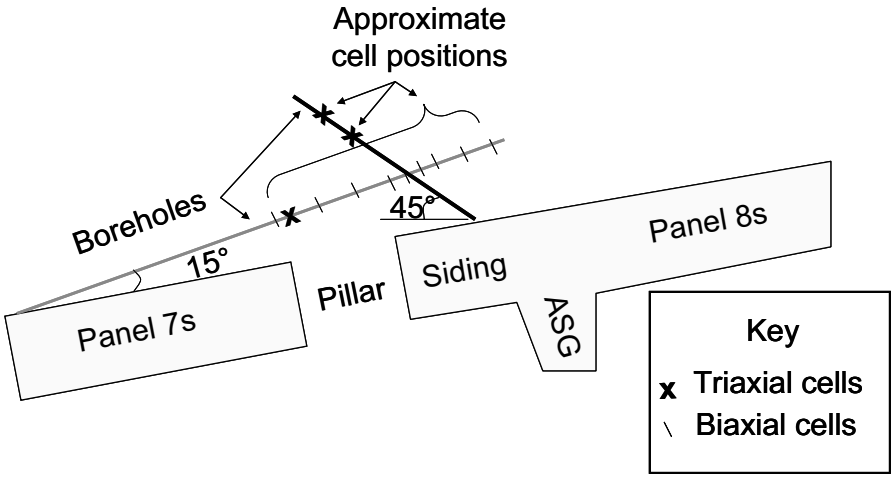

Figure 5 Section showing the instrumentation positions above the pillar (not drawn to scale)

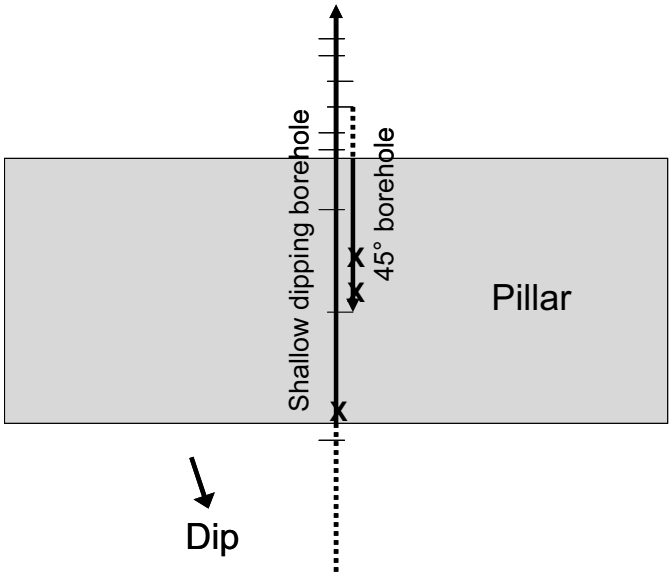

Figure 6 Plan view showing the instrumentation positions above the pillar (not drawn to scale). X=triaxial cells, -=biaxial cells

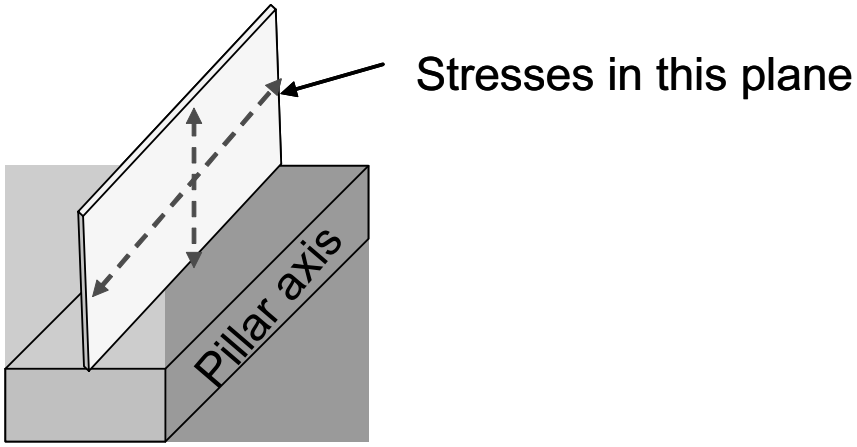

Figure 7 Sketch of a pillar showing the plane in which the 2D residual stress measurements were made

The measurements in the shallow-dipping hole ranged in height from 1.9 m to 3.7 m above the pillar. The intention was to measure vertical stress with a set of closely spaced cells. However, an obliquely oriented discontinuity prevented some measurements on the down-dip side of the pillar.

Two triaxial cells were installed in a borehole drilled up at 45°, from the up-dip panel, at heights of 3.8 m and 4.1 m above the pillar. These measurements allowed a much broader overview of the stress condition of the whole pillar, by virtue of their height above the pillar.

4 Instrumentation results

The strains provided by the stress cells were unusually large. This corresponded to the non-linear stress-strain relationship of the host rock shown in Figure 8. In particular, the high measured strains were accounted for by the low modulus shown by the uniaxial compressive strength (UCS) test at low stress.

The non-linear stress-strain relationship meant that the normal elastic constants (Tangential Modulus, *E,* and Tangential Poisson's Ratio, *v*) could not be used to evaluate the stress measurements.

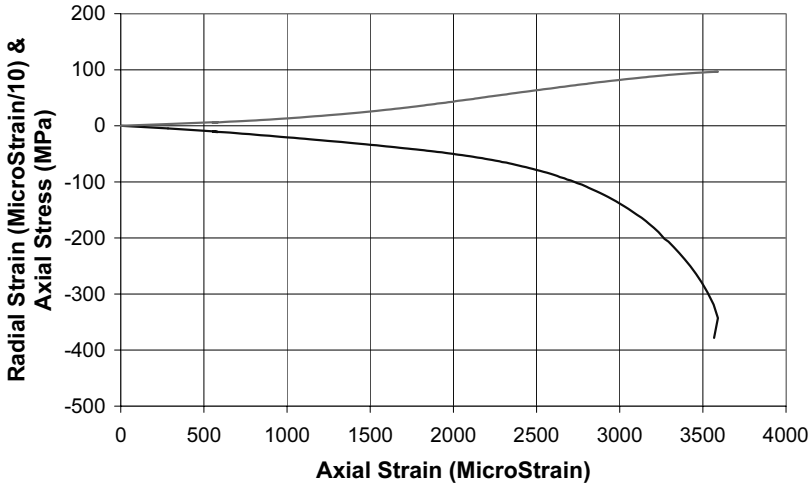

Figure 8 Stress-strain curve of the anorthosite rock above the instrumented pillar, provided by a laboratory UCS test

Further analysis and microscope work established that the behaviour was influenced by open micro-cracks. Thus, in theory, once the cracks are closed the material should behave in a normal, linear elastic manner. However, in the case of the UCS tests, the onset of failure occurred before the cracks were fully closed. The doorstoppers were, therefore, evaluated using a biaxial test, performed on specially prepared doorstopper samples as shown in

Figure ***9*** and Figure 10 respectively.

Unfortunately the coupling between the sample and the loading jaws was not good, which resulted in additional strain for the applied load at very low stress. The final solution incorporated a combination of both the biaxial and UCS tests.

Figure 9 Mechanical biaxial test apparatus for Doorstoppers

Figure 10 Specially prepared doorstopper sample

The effects of the stress concentrations at the ends of the boreholes were extracted from the measurements using reworked versions of the Vreede[4] equations for stress concentrations at the blind end of a borehole (Equations 1 to 3).

$$\sigma_y = \left(\frac{a}{(b^2 - a^2)}\right)\left[\overline{\sigma_x}\left(\frac{b}{a}\right) - \overline{\sigma_y} + c\sigma_z\left(1 - \frac{a}{b}\right)\right] \qquad \textbf{1}$$

$$\sigma_x = \frac{\overline{\sigma_x} - b\sigma_y - c\sigma_z}{a} \qquad \textbf{2}$$

$$\tau_{xy} = \frac{\overline{\tau_{xy}}}{(a-b)} \qquad \textbf{3}$$

Where: $\overline{\sigma_x}$, $\overline{\sigma_y}$ and $\overline{\tau_{xy}}$ are the measured stresses in the x and y directions.

The a, b and c-values for the non-linear elastic material were determined from FLAC[5] modelling. Their relationship to the Poisson's Ratio (v) is shown in the following equations.

$$a = 1.33 + 0.1\upsilon \qquad \textbf{4}$$

$$b = -0.13 + \frac{\upsilon(1 - 1.5\upsilon + 5\upsilon^2)}{3} \qquad \textbf{5}$$

$$c = 0.37 - 1.1\upsilon \qquad \textbf{6}$$

The triaxial cells were evaluated using the biaxial test apparatus shown in Figure 11. The stress concentrations on the inside of the hollow cylinder used in the tests meant that the radial and axial strains had to be evaluated separately for the non-linear material. A list of all the stress results is shown in Table 1. The triaxial cell results are in bold.

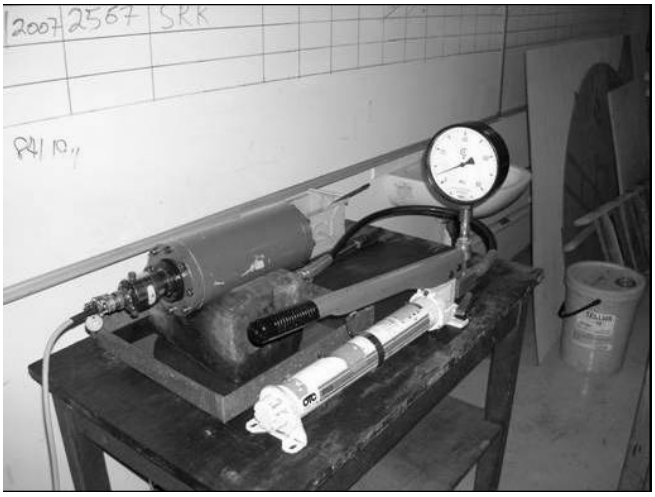

Figure 11 Test apparatus for loading triaxial cells

Table 1 Stress measurement results

Distance from pillar edge (m)	**Height above pillar (m)**	**Error in strain measure. (%)**	**Vertical stress (MPa)**
-0.29	1.93	6.8	9.4
0.02	**2.02**	**3.1**	**22.0**
1.99	2.55	5.7	95.6
2.79	2.76	1.3	67.2
3.34	2.91	-	59.5
4.71	3.27	4.7	1.0
5.11	3.38	5.1	0.6
5.47	3.48	8.2	0.1
6.41	3.73	6.1	0.5
1.95	**3.76**	**8.2**	**36.2**
1.68	**4.12**	**7.7**	**26.7**

5 Interpretation of the stress results

The stresses measured above the pillar represented a fraction of the stress on the plane of the top contact of the pillar. The stress distribution across the pillar itself was calculated using a smoothed, corrected inverse matrix of Boussinesq equations[6] (7), based on the measurements in the shallow-dipping borehole. An adjustment to the position of the stress measurements was necessary because the inverse matrix of the raw measurements predicted the peak stress to lie on the up-dip edge of the pillar. The observed fracturing clearly showed that was not the case. The Boussinesq equations assume that the host rock is elastic:

$$\sigma_{zz} = \sum_{i=1}^{n}\left[\frac{3A_i}{2\pi} \times \frac{z_i^3}{(x_i^2 + y_i^2 + z_i^2)^{5/2}}\, p_{zi}\right] \qquad \textbf{7}$$

Where: σ_{zz}= stress at a point in space;
A_i= Area of the grid "*i*"; p_{zi}= Vertical stress carried by the grid "*i*".

For the purposes of the calculations, the reef and measurements were rotated by 10° so that the top surface of the pillar could be considered horizontal. A plan view of the Boussinesq co-ordinate system used across the top boundary of the pillar is shown in Figure 12. The pillar was divided into 0.5 m x 0.5 m blocks as shown in the figure. The grid enabled multiple stresses to be considered across the pillar.

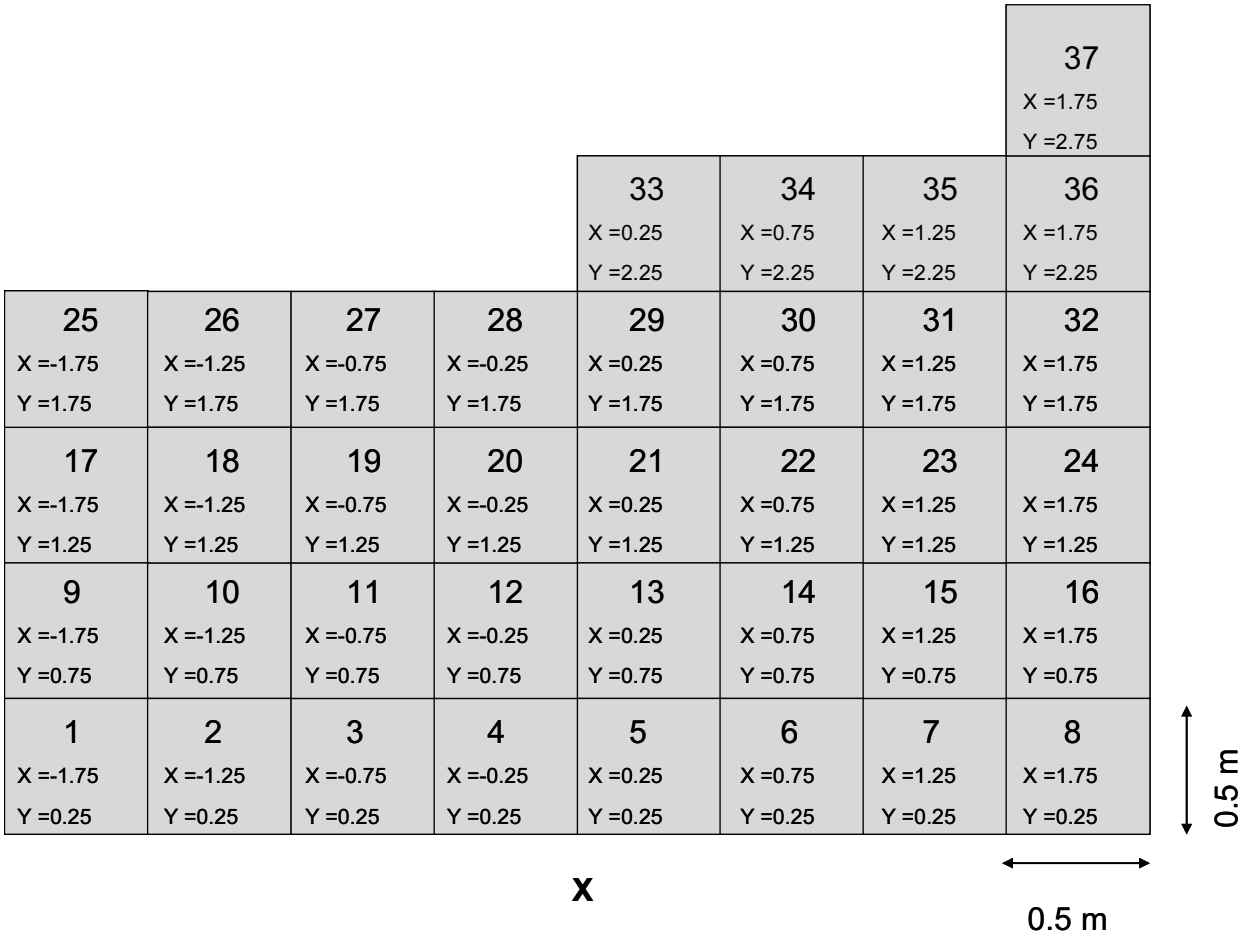

Figure 12 Plan view of the grid layout across the pillar for Boussinesq evaluation. The origin is the centre of the bottom (down-dip) edge. The bold "X" position (below grids "4" and "5" in the figure) represents the approximate position of the first stress measurement

The reference point used for the evaluation of the stress measurements was the centre of the down-dip edge of the pillar (the bottom edge in Figure 12). The matrix inversion of the "adjusted" stresses provides the estimated stress distribution across the pillar. While other measurements made around the pillar showed that it had failed, the Boussinsq evaluations suggest that the central core of the pillar is still carrying 2100 MPa. This high stress is unlikely as the physical conditions surrounding the pillar suggested a reasonably low stress environment after failure, with a stable hangingwall adjacent to the pillar (
Figure ***13***).

Figure 13 Down-dip side of the instrumented pillar. View away from face

Closely spaced vertical fractures were observed in shallow dipping boreholes drilled about 1.25 m above the adjacent pillars. These fractures were not observed in boreholes drilled 2 m above the pillars. Assuming that similar fractures exist over the instrumented pillar, and considering that shear stress cannot exist across these vertical planes, it is suggested that the stress on the top contact of the pillar would be the same as near the top of the discontinuities. This assumption was verified using a 2D Elfen model.

The model is a simple representation of a cross-section perpendicular to the pillar axis. The pillar and surrounding stope geometry were modelled in plane strain (Figure 14).

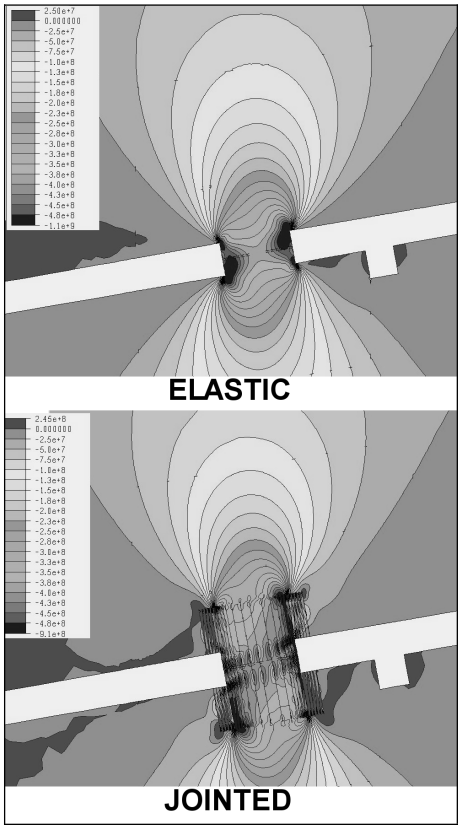

Figure 14 Vertical stress distribution for an elastic and a jointed model (Contour scales are identical)

The vertical load in the model was derived from the depth (1100 m) and overburden density (2800 kg/m^3). A k-ratio of 1.5 was assumed. An elastic reference model was constructed, consisting of a single continuum. To investigate the effects of jointing on stress, discrete joints were introduced into a second model. These reef-perpendicular joints extended 1.5 m above and below the pillar, and 0.5 m on either side. The joints were spaced 0.1 m apart at the pillar edge, the spacing increasing to 0.4 m in the centre. Figure 14 shows a comparison of the vertical stress distribution in the elastic and the jointed pillar.

It is clear that the presence of joints results in "channelling" of the vertical stress within the jointed region. Stresses measured at equivalent horizons from the pillar will be higher in the jointed hangingwall than those in the elastic model.

The modelled stresses at the in situ measurement positions were recorded in both models. These stresses and the stresses recorded at the centre of the pillar are presented in Figure 15 as "measurements" and "in-pillar stress distribution" respectively. Though the stress distributions are different, the magnitudes of the in-pillar stresses are not significantly influenced by the inclusion of joints. The stresses at the instrumentation positions, however, are increased by up to 59 % by the presence of jointing.

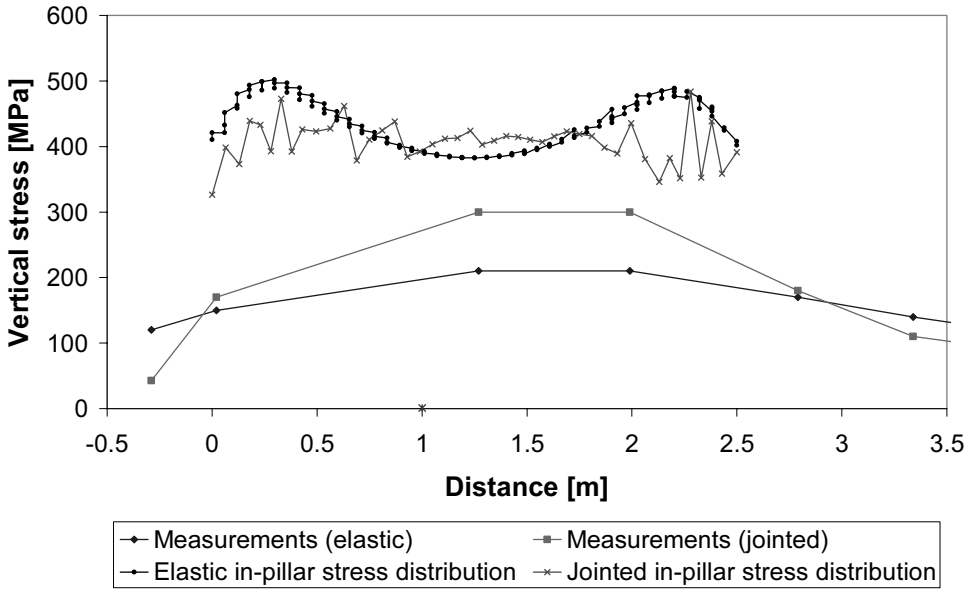

Figure 15 Distribution of stresses in the pillar centre and at in situ measurement positions for both the elastic and jointed models

A second Boussinesq evaluation was done assuming the heights of the measurements were 1.2 m closer to the pillar than the original investigation. In this evaluation the peak stress just up-dip of the pillar centre was shown to be 280 MPa. The evaluation also suggested an average pillar strength (APS) of 48 MPa. The stresses were determined on a grid size of 0.5 m x 0.5 m (Figure 12). A smaller grid is likely to have shown a slightly higher peak but a similar APS.

Both the peak and APS stresses are high for a failed pillar of width:height ratio 2.1:1. However, the pillar height was less than 0.5 m high in places on the up-dip side (Figure 4), which may have caused the pillar to carry a higher load on this side (Figure 16). The low height of the 2.5 m wide siding may have affected the effective width:height ratio, thus accounting for the high residual strength. The high density of fracturing in the hangingwall suggests that the pillar was carrying a high stress, probably at some stage before the siding was cut. Similar fracturing was observed on the down-dip side where the fractured sidewall of the pillar had fallen away.

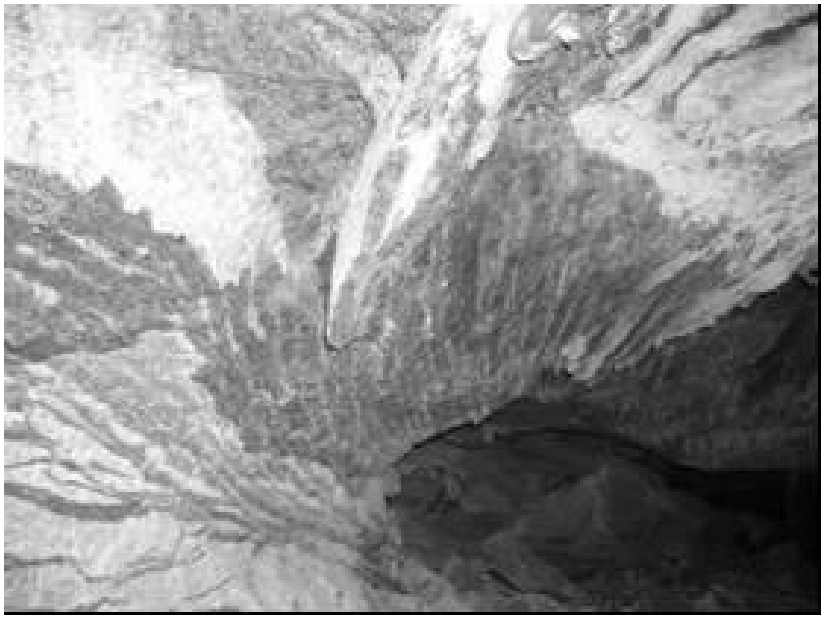

Figure 16 Up-dip side of the instrumented pillar. View towards face

The matrix inversion of the "adjusted" stresses in the final Boussinesq evaluation is compared to the measurements in Figure 17. Figure 18 shows the stress profile across the pillar that provides the adjusted curve shown in Figure 17.

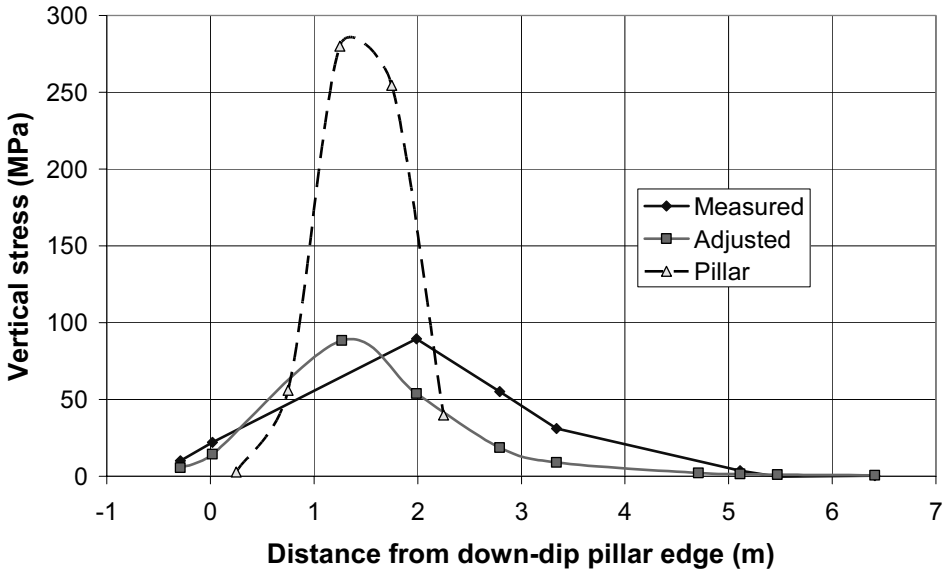

Figure 17 Stress profiles across the centre of the pillar, comparing the measured to the calculated

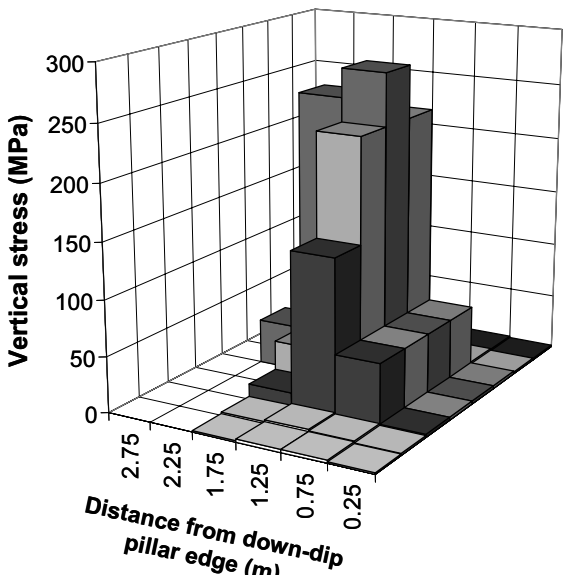

Figure 18 Stress profile across the pillar (provided by the Boussinesq inverse matrix)

Further analyses were done using the Boussinesq solution for shear stress[6] (8) to see if the measured off-centre peak stress could be explained by the presence of shear stresses. The evaluation reduced the peak stress slightly but did not succeed in adjusting its position.

$$\tau_{yz} = \sum_{i=1}^{n}\left[\frac{3A_i}{2\pi} \times \frac{y_i z_i^2}{(x_i^2 + y_i^2 + z_i^2)^{5/2}} p_{zi}\right] \qquad \textbf{8}$$

6 Discussion

No reasonable combination of Boussinesq stresses could simulate the off-centre peak stress shown by the measurements in the shallow-dipping hole. The positions of the measurements were therefore adjusted (Figure 17) so that the peak stress on the pillar elevation was just up-dip of the centre (Figure 18). Boussinesq back-analysis of the resultant pillar stress profile (Figure 17) did not provide a good correlation to the measurements in the 45° borehole. However, the magnitude of the peak stresses calculated from the back-analysis coincided with the measured values obtained in the 45° borehole. Since the instruments in the 45° borehole were directly above the peak measurements in the shallow-dipping borehole, the back analysis indicates that the peak stress in the shallow-dipping borehole was in fact located up-dip of the pillar centre, as measured. The back-analysed results (adjusted to coincide with the measured peak in Figure 17) and the measurements are shown in Table 2. If the measurement positions in the shallow-dipping borehole were wrong, then the back-analysed results in Table 2 would have been lower and the stress difference between the two results would also have been less. The good correlation between the measurements in the two boreholes also suggests that a higher stress was not present between the measurements at 0.2 m and 1.99 m (Table 1).

Table 2 Comparison between the measured and back analysed stresses in the 45° hole

Height above pillar (m)	Measured (MPa)	Back-analysed (MPa)	Diffe-rence %
3.76	26.7	26.3	1.5
4.12	36.2	33.8	6.6

As the difference between the calculated stresses was already less than the measurements, and good correlation was achieved between the calculated and measured values, the results from this hole suggest that the "measured" stresses in Figure 17 were correct. It also implies that the assumption of stress channelling between the vertical fractures is valid. In addition, the back analysis shows that the magnitudes of the "pillar" stresses in Figure 18 are approximately correct.

The stress distribution shown in Figure 18 is similar to the Wagner[7] profile for a failed coal pillar (profile 3 in Figure 19) except the peak in Figure 18 is significantly higher. Profile 3 in Figure 19 was for a pillar that had not reached the final residual strength. A higher peak would suggest that the pillar is further down the stress strain curve.

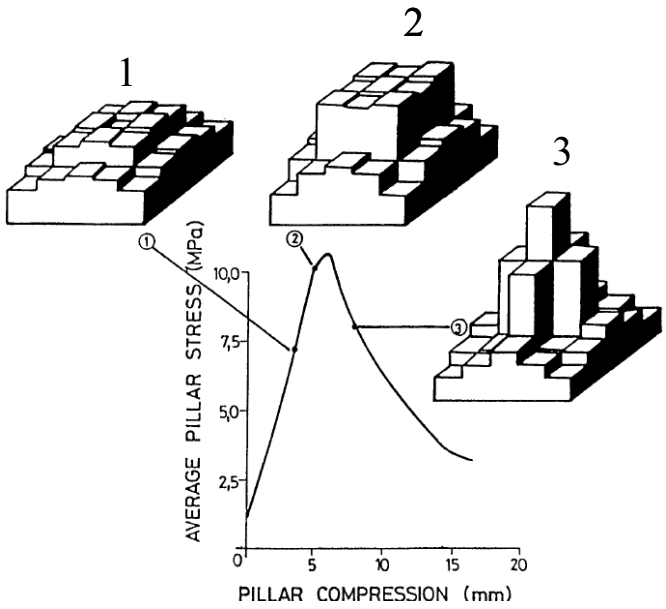

Figure 19 Wagner's[6] in situ tests on coal pillars, showing the stress profile across a pillar for three APS levels (1=elastic, 2=yield and 3=post-failure)

The relatively high peak suggested by the Boussinesq evaluation, considering that the pillar width:height ratio was only 2.1:1, indicates that the residual strength may not have been reached at the time of the measurements. In addition, instrument-tation installed over

significantly wider pillars in the same stope showed lower final peak stresses than that measured over the 2.1:1 pillar, again implying that the residual had not been reached.

However, stress change was measured on the evaluated pillar from before pillar failure. The stress had dropped to the measured value 12 months prior to the profile measurements and remained unchanged while further mining took place. In addition, the observed pillar condition (
Figure ***13***), the stable hangingwall adjacent to the pillar and the significant closure measured up-dip and down-dip of the pillar show that the pillar is in an advanced stage of failure. It is therefore concluded that the pillar is in or very close to the residual condition. The location of the pillar when the siding was cut and good blasting appears to have resulted in an unfractured siding. This solid siding may have contributed to the unexpectedly high residual strength of the pillar.

The good correlation of the profile in Figure 18 to the Wagner[7] profile in Figure 19 suggests that this profile is a reasonable representation of the state of stress within the pillar. As the up-dip height of the pillar was narrower than the down-dip side, the peak would be expected on the up-dip side of the pillar centre but not on the up-dip face as suggested by the measurements. A possible explanation for the shift in the measured peak is that a more complex fracture arrangement exists above the pillar than shown in Figure 14. The presence of a steeply-dipping joint oriented obliquely to the pillar and cutting through the borehole between measurements 2 and 3 (Table 1) may also have influenced the stress distribution in the hangingwall.

6 Conclusions and recommendations

The residual strength of the crush pillar with a width of 2.5 m was successfully determined from a series of stress measurements in two boreholes and a Boussinesq matrix inversion. The case study showed a residual strength of 48 MPa. The calculated peak stress was surprisingly high at 280 MPa. The stress condition is suspected to be abnormal due to the pillar geometry on the up-dip side and the stiff loading conditions under which failure took place. In order to get a more realistic evaluation of residual strength, a series of such measurements are recommended to establish a range of residual strengths for narrow crush pillars. These measurements should also be done on different mines to determine if and how siding dimensions, rock type and k-ratio influences the residual strength.

7 References

1. Korf, C.W. 1978. Stick and pillar support on Union Section, Rustenburg Platinum Mines. *Association of Mine Managers of South Africa*. pp 71-82.
2. Roberts, D.P., M.K.C. Roberts, A.J. Jager and S. Coetzer. 2005. The determination of the residual strength of hard rock crush pillars with a width to height ratio of 2:1. *J. South African Inst. Min. and Met.* Vol 105: pp 401-408.
3. Watson, B.P., Roberts, M.K.C., Nkwana, M.M., Kuijpers, J., Van Aswegen, L. 2007. The stress-strain behaviour of in-stope pillars in the Bushveld Platinum deposites in South Africa. *J. South African Inst. Min. and Met.* Vol 107:

4. Vreede, F.A., 1991. Algorithms for the least square equations used in virgin stress measurement. *Internal CSIR report EMA-1 9116.*
5. Itasca consulting group, inc. 1993 Fast Lagrangian Analysis of Continua (FLAC), Vers. 3.2. *Minneapolis Minnesota USA*.
6. Poulos, H.G. and E.H. Davis. 1974. *Elastic solutions for Soil and Rock Mechanics.* J Wiley& Sons. N.
7. Wagner, H., 1980. Pillar design in coal mines. *J. South African Inst. Min. and Met.* January. pp 37-45